THE JOURNAL OF BIOLOGICAL CHEMISTRY
Vol. 278, No. 40, Issue of October 3, pp. 38276–38286, 2003
Printed in U.S.A.

Regulation of the Epithelial Na^+ Channel by Cytosolic ATP*

Received for publication, July 7, 2003
Published, JBC Papers in Press, July 22, 2003, DOI 10.1074/jbc.M307216200

Toru Ishikawa‡§, Chong Jiang¶, M. Jackson Stutts‖, Yoshinori Marunaka, and Daniela Rotin¶‡‡**

*From the ‡Department of Biomedical Sciences, Graduate School of Veterinary Medicine, Hokkaido University Sapporo 060-0818, Japan, ¶The Hospital for Sick Children, Program in Cell Biology, and the Department of Biochemistry, University of Toronto, Toronto, Ontario M5G 1X8, Canada, the **Departments of Molecular Cell Physiology and Respiratory Molecular Medicine, Graduate School of Medical Sciences, Kyoto Prefectural University of Medicine, Kyoto 602-0841, Japan, and ‖Cystic Fibrosis/Pulmonary Research and Treatment Center, University of North Carolina, Chapel Hill, North Carolina 27599-7020*

The epithelial Na^+ channel (ENaC), composed of three subunits ($\alpha\beta\gamma$), is expressed in various Na^+-absorbing epithelia and plays a critical role in salt and water balance and in the regulation of blood pressure. By using patch clamp techniques, we have examined the effect of cytosolic ATP on the activity of the rat $\alpha\beta\gamma$ENaC (rENaC) stably expressed in NIH-3T3 cells and in Madin-Darby canine kidney epithelial cells. The inward whole-cell current attributable to rENaC activity ran down when these cells were dialyzed with an ATP-free pipette solution in the conventional whole-cell voltage-clamping technique. This run down was prevented by 2 mM ATP (but not by AMP or ADP) in the pipette solution or by the poorly or non-hydrolyzable analogues of ATP (adenosine 5′-*O*-(thiotriphosphate) and adenosine 5′-(β,γ-imino)triphosphate) in both cell lines, suggesting that protection from run down was mediated through non-hydrolytic nucleotide binding. Accordingly, we demonstrate binding of ATP (but not AMP) to αrENaC expressed in Madin-Darby canine kidney cells, which was inhibited upon mutation of the two putative nucleotide-binding motifs of αrENaC. Single channel analyses indicated that the run down of currents observed in the whole-cell recording was attributable to run down of channel activity, defined as NP_o (the product of the number of channels and open probability). We propose that this novel ATP regulation of ENaC may be, at least in part, involved in the fine-tuning of ENaC activity under physiologic and pathophysiologic conditions.

The amiloride-sensitive epithelial Na^+ channel (ENaC)[1] regulates a variety of physiological functions in different Na^+-transporting epithelia, such as those in the distal nephron, distal colon, lung epithelia, and duct cells of exocrine glands (1). ENaC is composed of three partially homologous subunits, α, β, and γ (2, 3). The physiological importance of ENaC has been underscored by the recent identification of either loss of function mutations in the channel leading to pseudohypoaldosteronism (PHA1) (4–6) or gain of function mutations causing pseudoaldosteronism (Liddle's syndrome), a hereditary form of arterial hypertension (7–9). Moreover, abnormally high ENaC activity has been associated with cystic fibrosis due to loss of the normal inhibitory effect of CFTR on ENaC (10–13), and gene targeting of αENaC in mice led to newborn death from pulmonary edema (14).

The activity of ENaC is tightly regulated not only by various hormones such as aldosterone and vasopressin but also by intracellular factors via mechanisms that are not yet fully understood (1). A mechanism by which the activity of ENaC is regulated in native Na^+-transporting epithelia is called the "feedback inhibition," which is defined as channel down-regulation due to the transport of Na^+ across the apical membrane and its accumulation intracellularly (1). This mechanism would allow cells to adjust optimal Na^+ movement across the apical membrane, thereby protecting themselves from Na^+ load and the energy consumption required to maintain Na^+ transport. Previous patch clamp studies in native Na^+-absorptive epithelia have shown that the feedback inhibition involves changes in intracellular factors, including membrane potential, cytosolic pH, Ca^{2+}, and Na^+ concentrations, and cell metabolism (1). Furthermore, in recent studies using both molecular biological and electrophysiological techniques, cytosolic pH, Na^+, and/or Ca^{2+} concentration have been also shown to affect the activity of the cloned rENaC when expressed in different heterologous expression systems (15–20), although these cytosolic factors may not act on the ENaC protein directly (18).

Focusing on the relationship between cell metabolism and Na^+ channel activity, Palmer *et al.* (21) and Garty *et al.* (22) observed that inhibition of cell metabolism decreased the apical membrane Na^+ permeability in the toad urinary bladder, although it is not known whether metabolites such as ATP were responsible for this effect. Frindt *et al.* (23) also suggested a role for metabolic changes in mediating negative feedback regulation of amiloride-sensitive Na^+ channels in rat cortical collecting tubules; they found that increasing Na^+ entry into cells by the addition of cAMP led to a decrease in channel activity in cell-attached patches, where the channels were apparently pro-

* This work was supported in part by grants-in-aid for Scientific Research C from the Ministry of Education, Science, Sports and Culture of Japan (to T. I.), by Yamada Science Foundation (to T. I.), by a grant from the Akiyama Foundation (to T. I.), by the Canadian Cystic Fibrosis Foundation (to D. R.), by the Canadian Institute of Health Research (to D. R.), by the Human Frontier Science Program (to D. R.), by the Kidney Foundation of Canada (to Y. M.), by a grant from the Ministry of Education, Science, Sports and Culture of Japan (International Scientific Research Program) (to Y. M.), and by a grant from the International Human Frontier Science Program (to D. R). The costs of publication of this article were defrayed in part by the payment of page charges. This article must therefore be hereby marked "*advertisement*" in accordance with 18 U.S.C. Section 1734 solely to indicate this fact.

§ To whom correspondence should be addressed: Laboratory of Physiology, Dept. of Biomedical Sciences, Graduate School of Veterinary Medicine, Hokkaido University, Sapporo 060-0818, Japan. Tel.: 81-11-706-5200; Fax: 81-11-706-5202; E-mail: torui@vetmed.hokudai.ac.jp.

‡‡ Supported by a Canadian Institutes of Health Research Scientist award.

[1] The abbreviations used are: ENaC, epithelial Na^+ channel; MDCK, Madin-Darby canine kidney cells; ATPγS, adenosine 5′-*O*-(thiotriphosphate); AMP-PNP, adenosine 5′-(β,γ-imino)triphosphate; rENaC, rat ENaC; HA, hemagglutinin; WT, wild type; GDPβS, guanyl-5′-yl thiophosphate; GTPγS, guanosine 5′-3-*O*-(thio)triphosphate; CFTR, cystic fibrosis transmembrane regulator; NB, nucleotide binding.

tected from the stimulatory effects of the nucleotide, and that inhibition of the Na^+-K^+-ATPase by ouabain prevented the inhibition of channel activity. The authors concluded that accumulation or depletion of metabolic substrates could play at least a partial role in regulating Na^+ channels, especially during times of metabolic stress. In accord, an earlier study had demonstrated decreased amiloride-sensitive Na^+ transport across bronchial epithelia following metabolic poisoning, which presumably caused ATP depletion (24). Recently, Chraïbi *et al.* (25) have identified a novel N-terminal splice variant, which deletes 49 amino acids in the N-terminal region of the αENaC. When co-expressed with the β- and γENaC subunits in *Xenopus* oocytes, the corresponding N-terminal deletion mutant of the αENaC produces significantly smaller amiloride-sensitive Na^+ currents than those with the wild type subunit. This smaller current was most likely attributable to a decrease in the overall open probability of active channels but not in single channel conductance or in surface expression of the channel (25). Because the N-terminal region contains a consensus nucleotide-binding motif (G*X*G*X*G motif), these observations together with those on native tissues have led us to hypothesize that a direct binding of cytosolic nucleotides such as ATP to the αENaC may be involved in a regulation of the channel activity.

By using patch clamp techniques, we have shown here for the first time that rENaC heterologously expressed in both NIH-3T3 fibroblasts and MDCK epithelial cells are regulated by cytosolic ATP, which is likely mediated by non-hydrolyzable nucleotide binding to rENaC itself (most likely directly) rather than by a hydrolytic mechanism.

EXPERIMENTAL PROCEDURES

rENaC Expressing NIH-3T3 and MDCK Cells—NIH-3T3 fibroblasts (3T3 cells) expressing heterologous rat $\alpha\beta\gamma$ENaC (rENaC, untagged) were previously generated by stably transfecting cells with a retrovirus expression vector (10). MDCK cells ectopically expressing untagged rENaC were described previously (10, 16). MDCK cells stably expressing HA-tagged αrENaC were described earlier (26), and those expressing all-tagged ENaC ($\alpha_{HA}\beta_{myc.T}\gamma_{FLAG}$-ENaC) have been described recently (27). Mutant HA-tagged αrENaC (Δ2NB) bearing Gly to Ala mutations in all glycines of the 2 putative nucleotide-binding motifs (GLGKG→ALAKA at the N terminus, and GRGARG→ARAARA at the C terminus) was generated using a QuickChange mutagenesis kit (Stratagene). The HA-αrENaC(Δ2NB) mutant was then stably transfected into MDCK cells, as described earlier for the HA-αrENaC(WT) cell line (26). Expression of the untagged ENaC subunits was confirmed by immunoprecipitation of the metabolically labeled channel using antibodies directed against each subunit (10)[2] and of the tagged ENaC was confirmed using the appropriate anti-tag antibodies in a Western blot. Cells were maintained in Dulbecco's modified Eagle's medium with 10% fetal bovine serum, penicillin (100 units/ml), streptomycin (100 μg/ml), G418 (0.3 mg/ml), and amiloride (10 μM) as described elsewhere (10, 16, 26) (and with hygromycin (100 μg/ml) + puromycin (5 μg/ml) for the all-tagged ENaC ($\alpha_{HA}\beta_{myc.T}\gamma_{Flag}$-ENaC) expressing MDCK cells). For patch clamp experiments, cells were seeded at low density on a cover glass, grown for 2–4 days. The 3T3 cells were induced with 2 mM butyrate (overnight), and the untagged rENaC-expressing MDCK cells with 1 μM dexamethasone and 2 mM butyrate (overnight) prior to patching, as described previously (10, 16). For binding experiments, the HA-tagged αrENaC-expressing MDCK cells were induced with 1 μM dexamethasone (overnight) and the all-tagged rENaC-expressing MDCK cells with 1 μM dexamethasone and 2 mM butyrate (overnight) prior to the experiments.

Patch Clamp Analyses—Cells grown on cover glass were rinsed with an appropriate NaCl-rich bath solution (see below), and then were transferred to a chamber mounted on an inverted microscope. Current recordings were made from 3T3 cells and MDCK cells using the standard whole-cell configuration of the patch clamp technique (28). The patch clamp pipettes, which were pulled from glass capillaries (LG16, Dagan, Minneapolis, MN) using a horizontal puller (model P-97, Sutter Instrument, San Rafael, CA) or a vertical puller (model PP-830, Narishige, Tokyo, Japan), had resistances of ~2–3 megohms when filled with a standard cesium glutamate-rich solution described below.

An Axopatch-1D patch clamp amplifier (Axon Instruments, Union City, CA) was used to measure whole-cell and single channel currents. The reference electrode was Ag/AgCl electrode, which was connected to the bath via an agar bridge (10 mg/ml) filled with a NaCl-rich bathing solution. The amplifier was driven by pClamp 6 software to allow the delivery of voltage step protocols with concomitant digitization of the whole-cell currents. The whole-cell currents were filtered through an internal four-pole Bessel filter at 1 kHz and sampled at 2 kHz.

Current-voltage (I-V) relations were studied using 10-mV voltage pulses, each of 400-ms duration, delivered at voltages ranging between −180 and +50 mV, and voltage pulses were separated by 3–10 s during which the cell potential was held at either −40 or 0 mV. Steady-state whole-cell currents were measured at 350 ms from the start of each voltage pulse. For kinetic analysis of the amiloride-sensitive whole-cell currents, most relaxations were fitted with a single exponential using a least squares method as described elsewhere (16).

As an alternative to voltage steps, voltage ramps were applied in the whole-cell experiments where the time course of changes in the current was examined. Typically, the command voltage was varied from −180 to −0 mV or from −140 to either 0 or +40 mV over a duration of 800 ms every 10 or 30 s as described in the text. We used this protocol to monitor rENaC activity because it was easily possible to identify any appearance of other conductances. Subsequently, we used two criteria to reject cells as having an abnormally large leakage conductance after whole-cell dialysis: (i) linear instantaneous I-V relation, and (ii) the reversal potential of the current was close to zero. In experiments with MDCK cells, the command voltage was varied from −100 to +20 mV over a duration of 400 ms every 30 s. Amiloride-sensitive currents were estimated under each condition by subtraction of currents measured under identical conditions except for the addition of 10 μM amiloride.

The capacitance transient current in most experiments was compensated by using the Axopatch-1D amplifier. The cell capacitance was 42.6 ± 1.2 pF (n = 222). The series resistance (R_s) in these studies, which was 11.9 ± 0.4 megohms (n = 222), was not compensated. The pipette potential was corrected for the liquid junction potentials between the pipette solution and the external solution and between the external solution and the agar bridge, as described by Barry and Lynch (29).

Single channel activity was recorded in the outside-out patch configuration (28). By convention, for outside-out patches, the intracellular potential corresponds to the pipette potential, and downward single channel currents (carried by Li^+ in the present study) correspond to Li^+ flux from the extracellular to the intracellular side of the membrane. Single channel currents were filtered at 50–100 Hz with an internal four-pole Bessel filter, sampled at 1–2 kHz, and stored directly into the computer's hard disk through the TL-1 DMA interface or Digidata 1200 interface (Axon Instruments, Foster City, CA). Subsequent current analysis was performed using programs supplied with both pClamp 6 and Axograph 3 softwares (Axon Instruments). Because all patches studied in the present study contained multiple channels (up to several tens of channels), we calculated the NP_o product (N = number of channels, P_o = open probability) as : $NP_o = I_{ENaC}/i$ where I_{ENaC} is the current resulting from ENaC (= total current minus current with no channel open, which was evaluated in the presence of 10 μM amiloride in the external solution) averaged over a recording period (every 0.5 min), divided by the unitary current (i) measured as the peak-to-peak intervals in the amplitude histogram or estimated as the mean of each current transition. This product could be calculated without making any assumptions about the total N in a patch or the P_o of a single channel. In our preliminary experiments, we could not routinely observe reliable channel activities in excised inside-out patches from 3T3 cells; hence, single channel recording using this configuration was not pursued.

The composition of the standard pipette and bath solutions was as follows. The pipette solution (pH 7.4) contained (in mM) cesium glutamate (100 or 120), CsCl (10), $MgCl_2$ (1), HEPES (10), EGTA (1 or 10), and adenosine nucleotide (Na_2-ATP) (0–10). In some experiments, ATP was replaced by equimolar ATP analogues (ATPγS or AMP-PNP) or by other nucleotides (UTP, GTP, AMP, and ADP). The pH of the solution was adjusted with CsOH at pH 7.4. The cells were initially immersed in a bath solution (pH 7.4) containing (in mM): NaCl (140), KCl (4.3), $MgCl_2$ (1), and HEPES (10). Before the establishment of whole-cell configuration, the bath solution was changed to the one (pH 7.4) containing (in mM) sodium glutamate, lithium glutamate, or potassium glutamate (145), $MgCl_2$ (1), and HEPES (10). The pH of the solution was adjusted with NaOH, LiOH, or KOH, respectively. All chemicals were of

[2] O. Staub and D. Rotin, unpublished data.

reagent grade and were obtained from Sigma.

All experiments were performed at room temperature (20–23 °C). Bath solution changes were accomplished by gravity feed from reservoirs. The results were reported as means ± S.E. of several experiments (n), and n refers to the number of cells patched in the different plate. Statistical significance was evaluated by using the two-tailed paired and unpaired Student's t test. A value of $p < 0.05$ was considered significant.

ATP-binding Experiments—For binding (pull down) experiments, MDCK cells expressing HA-αrENaC (WT or the Δ2NB mutant) or all-tagged rENaC ($\alpha_{HA}\beta_{myc.T}\gamma_{Flag}$-ENaC) were induced to express the ENaC subunits overnight and then lysed in lysis buffer (50 mM HEPES, pH 7.5, 150 mM NaCl, 1.5 mM $MgCl_2$, 1 mM EGTA, 0.5 or 1% Triton X-100, 2 mM phenylmethylsulfonyl fluoride, 20 μg/ml of each aprotinin, leupeptin, and pepstatin A). Lysates were then diluted in phosphate-buffered saline (containing also 1 mM phenylmethylsulfonyl fluoride, 10 μg/ml each of aprotinin, leupeptin, and pepstatin A, 5 mM EDTA, and 0.5 mM $NaVO_4$) to reduce Triton X-100 concentration to 0.15–0.20%. Equal concentrations (unless otherwise indicated) of ATP or AMP conjugated to agarose beads (Sigma) were then incubated with the diluted lysate for 1.5 h (4 °C) and then beads washed (3 times) with HNTG (20 mM HEPES, pH 7.5, 150 mM NaCl, 0.1% Triton X-100, 10% glycerol,) and phosphate-buffered saline (1 time). Proteins were then separated on a 7 or 10% SDS-PAGE and immunoblotted with anti-HA antibodies to detect αrENaC.

RESULTS

Electrophysiological Properties of rENaC Heterologously Expressed in NIH-3T3 Cells—A previous study has shown that αβγrENaC-expressing 3T3 cells, but not untransfected 3T3 cells, exhibit an amiloride-sensitive conductance (10, 11). By using the conventional whole-cell configuration with the standard cesium glutamate-rich pipette solution containing 2 mM ATP and lithium glutamate-rich bath solution, we first characterized in detail amiloride-sensitive macroscopic currents mediated by rENaC in this heterologous expression system. Fig. 1*A-c* shows the traces of the amiloride-sensitive whole-cell current obtained by digitally subtracting the whole-cell currents recorded in the presence of amiloride (10 μM) (Fig. 1*A-b*) from those in its absence (Fig. 1*A-a*) and indicates that an activation of the whole-cell current associated with membrane hyperpolarization was truly mediated by amiloride-sensitive conductance. Although the activation time constant did not change significantly at voltages between −184 and −104 mV (Fig. 1*B*: the values at −184 and −104 mV were 105.7 ± 13.9 ms (n = 11) and 114.4 ± 22.4 ms (n = 10), respectively), the relative amiloride-sensitive current amplitude was slightly voltage-dependent, so that the relative value was 1.37 ± 0.09 (n = 11) at −184 mV and 1.18 ± 0.06 (n = 10) at −104 mV ($p < 0.002$) (Fig. 1*C*).

We next examined the relative conductance sequence for various cations of the whole-cell currents. In these experiments, whole-cell currents were recorded in the presence of 150 mM Na^+, K^+, or Li^+ as the glutamate salt in the bathing solution. Fig. 1*D* summarizes these results. When the amiloride-sensitive Li^+ and Na^+ or Li^+ and K^+ currents were measured in the same cells, the corresponding currents at a command voltage of −100 mV were −1.54 ± 0.33 nA (n = 8) and −0.81 ± 0.17 nA (n = 8) or −1.35 ± 0.20 nA (n = 9) and 0.05 ± 0.03 nA (n = 9), respectively. The ratio of the amiloride-sensitive K^+ or Na^+ to Li^+ current at −100 mV was calculated to be −0.04 ± 0.02 (n = 9) or 0.55 ± 0.07 (n = 8). These results indicate that the amiloride-sensitive conductance is permeable to Li^+ and Na^+ but not to K^+.

We also characterized single channel conductance of rENaC expressed in NIH-3T3 cells in outside-out patches, which could be responsible for the amiloride-sensitive whole-cell currents. The patch pipette was filled with a cesium glutamate solution, and the bath contained lithium glutamate-rich solution as in the whole-cell experiments. Fig. 2*A* shows an example of such

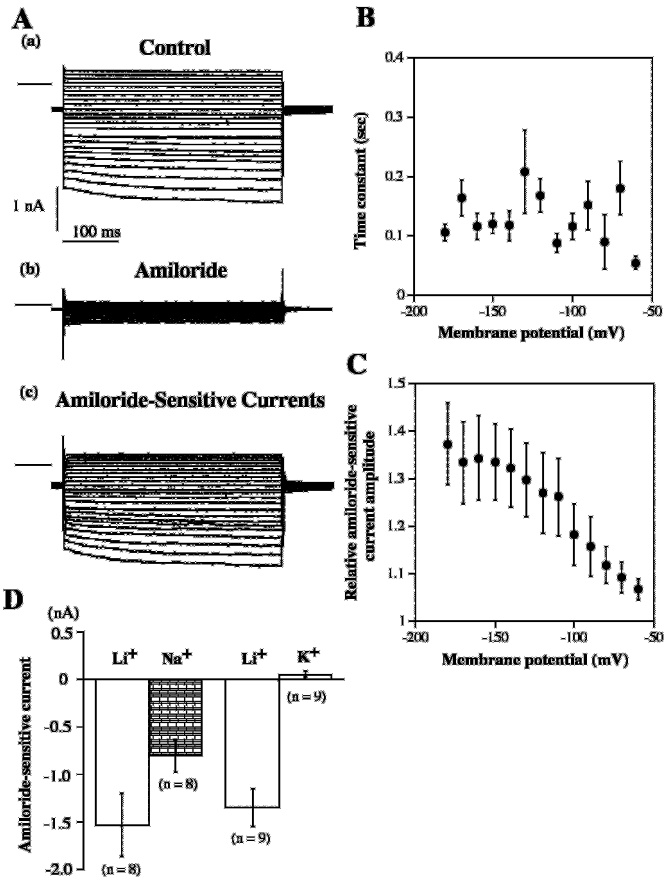

FIG. 1. **Voltage dependence of whole-cell Li^+ conductance in rENaC-expressing NIH-3T3 cells.** *A*, an example of tracings of the whole-cell currents before (*a*) and after (*b*) the addition of amiloride (10 μM) to the bath solution. *c*, tracings of amiloride-sensitive currents obtained from *a* and *b*. Hyperpolarizing and depolarizing pulses 400 ms in duration were applied from a holding potential of −44 mV to potentials between −184 and +46 mV in 10-mV intervals. The pipette was filled with a cesium glutamate-rich solution. Dependence of the relaxation time constant (*B*) and amiloride-sensitive current amplitude relative to that at −44 mV (*C*) on the membrane potential estimated from the whole-cell Li^+ current induced by voltage pulses from a resting potential of −44 mV. The relative amiloride-sensitive current amplitude is defined as described under "Experimental Procedures." Each point represents the mean ± S.E. of 3–11 experiments. *D*, comparison of amiloride (10 μM)-sensitive Li^+, Na^+, and K^+ currents in rENaC-expressing NIH-3T3 cells. Whole-cell currents were recorded in the presence of 150 mM Na^+, Li^+, or K^+ as the glutamate salt in the bathing solution. Amiloride-sensitive K^+ currents were measured in the presence of 1 mM $BaCl_2$ in the bath solution containing 150 mM K^+, because the cells exhibited a large inward whole-cell K^+ conductance. The blocker had little, if any, effect on ENaC activity when Li^+ was used as a charge carrier (data not shown). The amiloride-sensitive Na^+ and Li^+ currents were measured in the same cells. Data are the mean ± S.E. of 8 or 9 experiments.

experiments, demonstrating the presence of amiloride-sensitive single channel currents in an outside-out patch. In this patch, single channel current transitions with up to seven open levels could be observed, and application of amiloride (10 μM) reversibly abolished channel activity. Under these conditions, the single channel conductance for Li^+ or Na^+ was estimated to be 7.9 ± 0.5 pS (n = 8) or 3.9 ± 0.1 pS (n = 3), respectively. Consistent with the whole-cell experiments, we could not detect any current transition when K^+ was substituted for Li^+ (n = 7, data not shown) in the presence of 1 or 10 mM $BaCl_2$ in the bath solution. We also verified that the blocker did not affect the single channel conductance when Li^+ was used as a charge carrier (data not shown).

In single channel experiments, we also confirmed the obser-

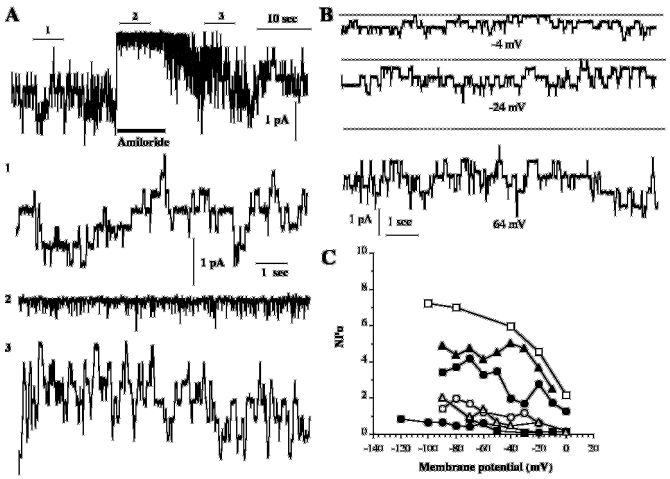

FIG. 2. *A*, an example of single channel activity recorded in an outside-out patch from rENaC expressed in 3T3 cells. The patch pipette was filled with cesium glutamate solution and the bath contained lithium glutamate-rich solution. Application of amiloride (10 μM), the period of which is indicated by *thick bar*, to the bath solution abolished channel activity. The *top trace* shows the time course of the amiloride effects. Three parts of the trace (*1–3*) are extended to display details of the channel activity. Holding potential was −24 mV. *B*, voltage dependence of single channel activity in outside-out patches. Tracings of a single channel inward current obtained from an outside-out patch. The channel activity defined as NP_o at a holding potential of −4, −24, and −64 mV were 1.54, 2.14, and 3.29, respectively. *C*, summary of 7 different experiments where NP_o was determined at various membrane potentials. Lines connect data obtained from the same patch. The patch pipette was filled with cesium glutamate solution, and the bath contained lithium glutamate-rich solution.

vation in the whole-cell patch clamp experiments (Fig. 1), demonstrating that channel activity is increased upon membrane hyperpolarization. Fig. 2, *B* and *C,* shows an example of such experiments and a summary of the results of 7 different experiments, respectively. Although the absolute value of NP_o was variable between each experiment, it was consistently increased upon membrane hyperpolarization (Fig. 2*C*). When NP_o value was normalized to a value of 1 at −24 mV, the relative NP_o was 2.54 ± 0.68 (n = 6) ($p < 0.01$) at −84 mV. Together, these results extend previous electrophysiological characterizations of rENaC stably expressed in 3T3 cells (10, 11) and show that the biophysical properties of the macroscopic and microscopic currents attributable to the activity of rENaC expressed in these cells were similar to those observed in native Na^+-transporting epithelia, such as rat cortical collecting tubule (1) and other heterologous expression systems such as *Xenopus* oocytes and MDCK cells (3, 16, 30).

Run Down of Whole-cell Na^+ Conductance in rENaC-expressing 3T3 Cells—In the course of our experiments, we noticed that the whole-cell currents attributable to rENaC activity exhibited a run down when the cells were dialyzed with a standard cesium glutamate-rich solution with no ATP. We first realized this phenomenon due to the small amiloride-sensitive whole-cell conductance detected in 3T3 cells expressing rENaC. Because in our initial experiments the measurement of whole-cell currents was started at least a few minutes after whole-cell dialysis, we thus performed a systematic time course experiment to examine if the Na^+ channel activity would run down during whole-cell dialysis. An example of such experiments is shown in Fig. 3*A*. Ramp command voltages were applied between −184 and −4 mV from a holding potential of −44 mV every 10 s. As shown in the figure, the inward whole-cell currents ran down and reached a steady-state level within 3 min. A residual whole-cell conductance was still completely amiloride-sensitive (Fig. 3*B*), and the whole-cell Li^+ conduct-

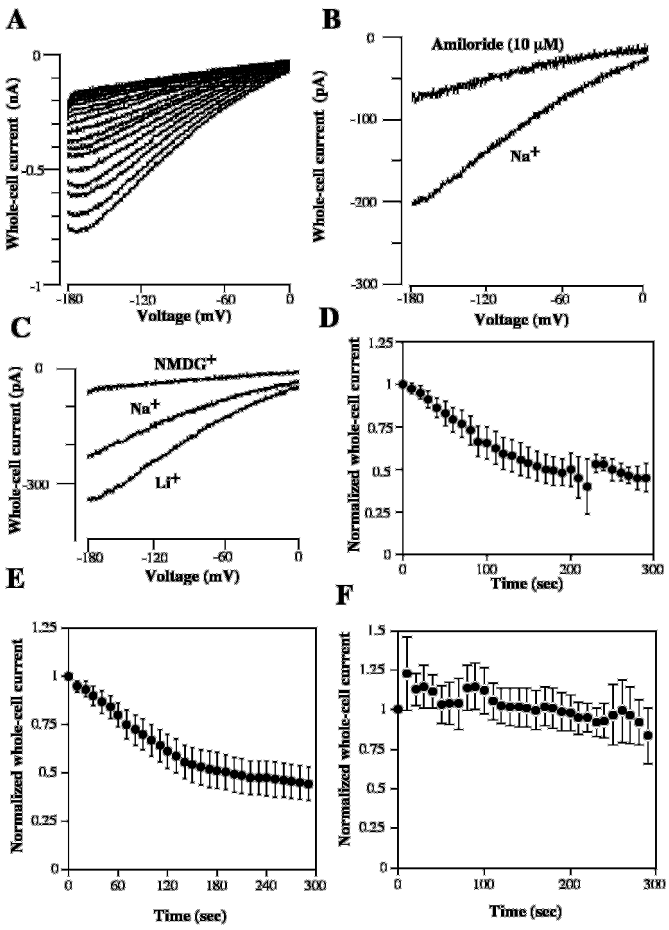

FIG. 3. *A,* an example of run down of the whole-cell inward current in 3T3 cells expressing rENaC. Ramp voltages were applied from −183 to −3 mV every 10 s. The holding potential was −43 mV. The pipette was filled with a cesium glutamate-rich solution with no ATP, and the bath solution contained sodium glutamate solution. Effects of amiloride (10 μM) (*B*) and replacement of 150 mM Na^+ with an equimolar Li^+ or $NMDG^+$ (*C*) in the bath solution on the residual currents after run down. Data were obtained from the same cell shown in *A*. *D*, summary of time course of changes in the inward current amplitude at −104 mV. The current amplitude was normalized to 1 with the initial measurements. Data represent the mean ± S.E. of 5 experiments. The patch pipette was filled with cesium glutamate solution (1 mM EGTA) with no ATP, and the bath contained sodium or lithium glutamate-rich solution. *E*, effects of increasing EGTA concentration to 10 mM in the pipette solution on the inward current at −104 mV. Currents were elicited by 800-ms voltage ramp between −144 and −4 mV from a holding potential of −44 mV every 30 s. The current amplitude was normalized to 1 with the initial measurements. Data represent the mean ± S.E. of 11 experiments. The patch pipette was filled with cesium glutamate solution (1 mM EGTA) with no ATP, and the bath contained a lithium glutamate-rich solution. *F*, effects of addition of ATP (2 mM) to the pipette solution on the inward current at −104 mV. Experimental protocol was same as in *E*. The current amplitude was normalized to 1 with the initial measurements. Data represent the mean ± S.E. of 5 experiments.

ance was greater than that of Na^+ (Fig. 3*C*). Furthermore, an activation of the whole-cell current was also observed when the membrane was strongly hyperpolarized (data not shown). We also confirmed in other sets of experiments that most of the inward currents under these conditions were amiloride-sensitive in cells that fulfilled the following criteria: (i) an inwardly rectifying instantaneous I-V relation, and (ii) an extrapolated reversal potential of the current was far from zero (usually greater than +30 mV). Under these conditions, total inward current at −104 mV was −1.92 ± 0.40 nA (n = 11). Amiloride-insensitive conductance measured just after whole-cell dialysis was only 13.5 ± 2.8% (n = 11) of the total inward current at −104 mV.

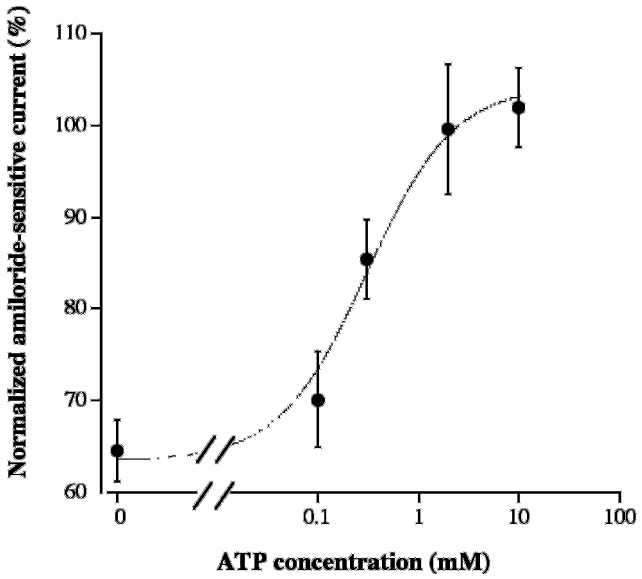

FIG. 4. **The effect of different concentrations of ATP (0–10 mM) in the pipette solution on the run down of the amiloride-sensitive currents.** Currents were elicited by 800-ms voltage ramp between −144 or −184 mV and −4 mV from 3T3 cells expressing rENaC. For comparison, the amiloride-sensitive current values 5 min after whole-cell dialysis were normalized to those measured at 0 min at −104 mV. Initial amiloride-sensitive current at −104 mV was −1.38 ± 0.27 nA (n = 16), −1.66 ± 0.24 nA (n = 18), −1.78 ± 0.32 nA (n = 13), −1.54 ± 0.24 nA (n = 14), or −1.30 ± 0.14 nA (n = 17) when the cells were dialyzed with a pipette solution containing 0, 0.1, 0.3, 2, or 10 mM ATP, respectively. Shown are mean ± S.E.

Fig. 3*D* shows the time course of run down of the inward current amplitude at −104 mV, which was normalized to the value at the initial measurement made within a few tens of seconds of formation of the whole-cell configuration. The normalized current amplitude within 3 min after whole-cell dialysis was decreased to 49.0 ± 8.6% (n = 5). These results suggest that activity of rENaC expressed in 3T3 cells runs down after whole-cell dialysis using a pipette solution containing no ATP.

Because it has been shown that an increase in cytosolic Ca^{2+} concentrations inhibits the activity of rENaC heterologously expressed in MDCK cells (16) and in *Xenopus* oocytes (19), we examined the possibility that cytosolic Ca^{2+} levels had not been clamped at a low enough concentration in 3T3 cells under the present experimental condition. We thus increased the concentration of EGTA in the pipette solution containing no ATP from 1 to 10 mM. As shown in Fig. 3*E*, however, there was little if any difference in the time course of run down between these two experimental conditions, so that the normalized current amplitude within 5 min after whole-cell dialysis was decreased to 44.3 ± 8.7% (n = 11). These results suggest that cytosolic Ca^{2+} does not play a role in the run down of rENaC.

Inclusion of ATP in the Pipette Solution Prevents Run Down of the rENaC Current—We next examined the effect of inclusion of ATP in the pipette solution. When 2 mM ATP was added to the pipette solution, the cells exhibited a stable whole-cell inward current even after 5 min of whole-cell dialysis (Fig. 3*F*). In order to characterize the ATP dependence of the run down, we performed other sets of experiments where cells were dialyzed with a pipette solution containing different concentrations of ATP (0–10 mM) (Fig. 4). To assess quantitatively the relationship between ATP concentration in the pipette solution and the run down, we measured the amiloride-insensitive inward current at the end of the experiments and subtracted it from the inward current. In separate experiments, we also ensured that the amiloride-insensitive current was stable during the experiments, so that the normalized amiloride-insensitive current amplitude 5 min after dialysis was 118.5 ± 14.3% (n = 7) of the initial level of the amiloride-insensitive current amplitude at −104 mV. The time-dependent decrease in inward current was dependent on the concentration of ATP in the pipette solution. The normalized current amplitude 5 min after whole-cell dialysis was 99.6 ± 7.1% (n = 13) of the initial level of the amiloride-sensitive current, which was significantly different from that observed with ATP-free solution (64.5 ± 3.4% (n = 16) ($p < 0.0003$). With ATP present in the pipette at 0.1 or 0.3 mM, inward current ran down and the current amplitude at −104 mV decreased to 70.1 ± 5.3 (n = 18) or 85.4 ± 4.3% (n = 13) of the initial amiloride-sensitive current level 5–6 min after dialysis of the cells. In contrast, at a concentration of 10 mM ATP, the inward current was stable after whole-cell dialysis, so that the normalized current amplitude at −104 mV was 102.0 ± 4.3% (n = 17). When the current amplitude (normalized to the initial level 5 min after whole-cell dialysis) was plotted against the pipette ATP concentrations, the K_d value was estimated to be ~0.31 mM (Fig. 4). These results suggest that cytosolic ATP affects the activity of ENaC.

ATP Hydrolysis Is Not Required for the Effect of ATP—Prevention of the run down by ATP observed in the whole-cell recordings could have at least two explanations. One is the modulation of ENaC function by protein kinases and/or through ATP hydrolysis as shown in the cystic fibrosis transmembrane regulator (CFTR). The other is modulation of ENaC activity through non-hydrolytic ATP binding to the channel itself or to an associated protein, as seen in other types of channels and transporters (31, 32). To distinguish between these two possibilities, we first examined the effect of removal of Mg^{2+} from the pipette solution on the inward current amplitude, because both protein kinases and ATPases require ATP with Mg^{2+} as a substrate. In the presence of 10 mM ATP, with or without Mg^{2+} (Fig. 5, *A* and *B*), the inward current did not run down, and the normalized inward current amplitude was 116.6 ± 16.2% (n = 8) of the initial level 5 min after dialysis (Fig. 5*B*). To ensure that free Mg^{2+} concentration in the cytosol was clamped to a low level after whole-cell dialysis, we further included 10 mM EDTA in the pipette solution containing no Mg^{2+} (Fig. 5*C*). Under these conditions, the whole-cell current was stable during the experiments, so that the normalized inward current amplitude 5 min after whole-cell dialysis was 105.0 ± 1.2% (n = 3) of the initial level.

We next investigated the effect of a poorly hydrolyzable ATP analogue, ATPγS (2 mM), and a non-hydrolyzable ATP analogue, AMP-PNP (2 mM). ATPγS or AMP-PNP (2 mM) were both effective at preventing the run down, and the normalized inward current amplitude at −104 mV was 94.2 ± 8.6 (n = 6) or 108.2 ± 15.0% (n = 10) of the initial level, respectively (Fig. 5, *D* and *E*). Taken together, these results are compatible with the notion that ENaC activity may be regulated by ATP through non-hydrolytic binding.

Effects of Other Nucleotides—To investigate the specificity of inhibition of rENaC run down by nucleotides, we examined the effect of dialyzing the cells with a pipette solution containing 2 mM AMP. A representative example of an experiment involving dialysis with 2 mM AMP is depicted in Fig. 6*A*, showing that AMP was unable to prevent the run down (normalized amiloride-sensitive current amplitude at −104 mV was 56.9 ± 5.2% (n = 14) of the initial level 5 min after onset of dialysis) (Fig. 6*B*). Likewise, ADP did not prevent the run down nor did 2 mM GTP or UTP (normalized amiloride-sensitive current amplitudes at −104 mV after 5 min of dialysis were 72.9 ± 2.6 (n =

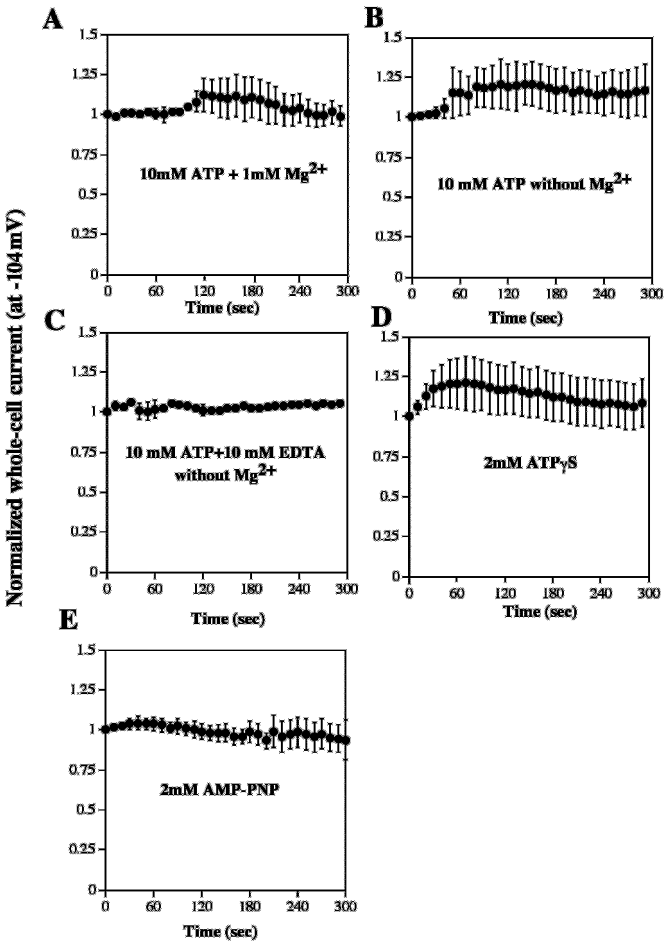

FIG. 5. Effects of removal of Mg^{2+} from the pipette solution (*B*) and of addition of EDTA (10 mM) to the pipette solution with no added Mg^{2+} (*C*). The control experiments with 1 mM Mg^{2+} is shown in *A*. The cesium glutamate-rich pipette solution contained 10 mM ATP and 10 mM EGTA, and the bath contained lithium glutamate-rich solution. Currents were elicited by 800-ms voltage ramp between −144 and −4 mV from a holding potential of −44 mV every 30 s. Data are the mean ± S.E. of 17, 8, or 3 experiments. Effect of the poorly hydrolyzable or the non-hydrolyzable ATP analogue, ATPγS (*D*) or AMP-PNP (2 mM) (*E*). Pipette contained cesium glutamate-rich solution, and the bath contained lithium glutamate-rich solution. Data are the mean ± S.E. of 6 or 10 experiments.

14), 71.7 ± 4.9 (n = 19), or 61.2 ± 4.7% (n = 14), respectively) (Fig. 6*C*).

Effects of Cytosolic ATP on the Voltage-dependent Activation of rENaC—We showed that rENaC heterologously expressed in 3T3 cells is activated by membrane hyperpolarization (Fig. 1) as shown in native rat cortical collecting duct cells (33, 34) and in rENaC heterologously expressed in MDCK (16). We next examined whether depletion of cytosolic ATP might change the voltage-dependent activation of rENaC. To do this, we dialyzed the cells with a pipette solution containing no ATP and compared the results with a voltage-dependent activation seen in cells dialyzed with 2 mM ATP (shown in Fig. 1). When the cells were dialyzed with a pipette solution containing no ATP, the relative amiloride-sensitive current amplitude was also shown to be slightly voltage-dependent, so that the relative value was 1.43 ± 0.07 (n = 7) at −184 mV and 1.19 ± 0.05 (n = 7) at −104 mV, respectively. These values were similar to those observed in the cells dialyzed with a pipette solution containing ATP (2 mM). These results suggest that voltage-dependent activation is not affected by cytosolic ATP.

Run Down of the Macroscopic rENaC Currents Is Not Associated with the Reduction in the Single Channel Conductance of rENaC—Because whole-cell current can be defined as the product of single channel conductance, number of channels (N), and open probability (P_o) of an individual channel, we first examined the possibility that the single channel conductance might be decreased upon ATP removal or other nucleotides replacement of ATP in the whole-cell experiments. To do this, we used an outside-out patch configuration, because under these experimental conditions, both cytosolic and extracellular environment should be the same as in whole-cell experiments. As summarized in Table I, there were little, if any, changes in the single channel conductance between the different experimental conditions, suggesting that a change in single channel conductance was not responsible for the results of the whole-cell experiments.

Run Down of the Macroscopic Currents Is Associated with Changes in Single Channel Activity of rENaC—We subsequently examined the effect of cytosolic ATP on ENaC activity at the single channel level. We used an outside-out patch configuration to examine directly whether cytosolic ATP concentration would affect the run down of channel activity seen in the whole-cell experiments described above. In the outside-out configuration, the identity of the channel could be verified by the reversible blocking effect of amiloride. This was especially important in the present study, because the patch membrane always contained multiple channels (up to several tens of channels). After the whole-cell configuration was established, outside-out patches were made, and channel activity was continuously recorded at a fixed membrane potential ranging from −10 to −50 mV for more than 5 min. Fig. 7 shows two examples of recording made in outside-out patches, either without ATP (Fig. 7*A*) or with 2 mM ATP (Fig. 7*B*). As evident, channel activity ran down during the experimental period when the pipette solution contained no ATP. The time course of changes in the relative NP_o is shown in Fig. 8*A*. NP_o value was normalized to 1 with the value of the initial 30 s. In 12 experiments, we observed that channel activity (NP_o) decreased to 45.5 ± 6.9% of the initial value within 4 min (Fig. 8*B*). Similar experiments were repeated using different concentrations of ATP in the pipette solution. Fig. 7*B* represents an example of these experiments, where the cytosolic surface of the membrane was exposed to 2 mM ATP. The time course of changes in the relative NP_o is also shown in Fig. 8*A*. As seen in these figures, channel activity was relatively stable during the experiments (NP_o of 90.1 ± 9.4% (n = 15) of the initial value at 4 min after excision). When the pipette solution contained a higher concentration of ATP (10 mM), NP_o was 84.2 ± 5.8% (n = 10) of the initial value (Fig. 8*A*). We also examined the effect of ADP on the stability of channel activity in excised outside-out patches, and we showed that cytosolic ADP at 2 mM was unable to prevent channel run down (NP_o of 55.7 ± 12.9 (n = 7) of the initial value within 4 min) (Fig. 8*B*).

Run Down of rENaC Activity in MDCK Cells and Its Prevention by Cytosolic ATP and the Non-hydrolyzable ATP Analogue, AMP-PNP—Because the 3T3 cells are fibroblasts (which, with some exceptions (35), do not normally express ENaC), we investigated whether the ATP-dependent run down observed in these cells could also be observed in an epithelial cell. To this end, we used MDCK cells stably transfected with αβγ-rENaC, because (i) these are kidney epithelial cells, (ii) their electrophysiological properties had been extensively characterized (16), and (iii) our unpublished work has detected trace amounts of endogenous ENaC in these cells, suggesting that they possess the proper cellular environment for ENaC regulation. Although in our previous study (16) we used a conventional whole-cell patch clamp configuration with an ATP-free pipette solution, in that earlier study we only characterized the whole-

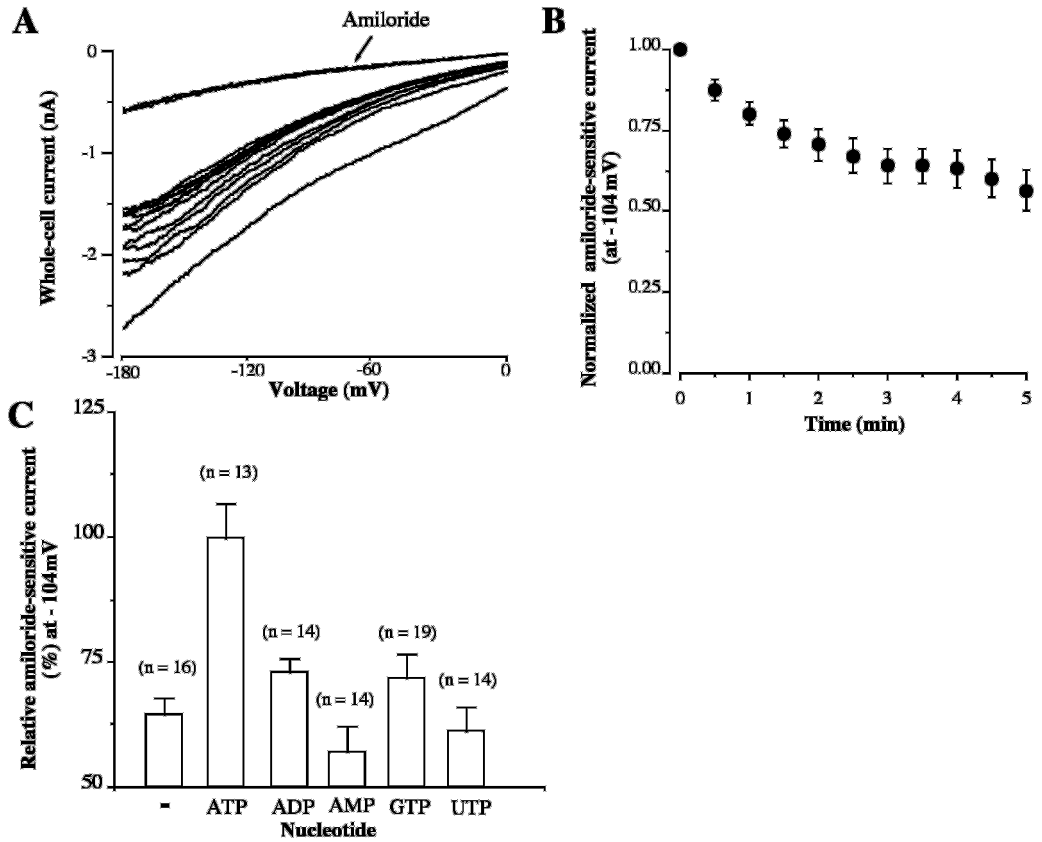

FIG. 6. **Effects of different nucleotides on the run down of the amiloride-sensitive currents.** *A*, representative tracings of whole-cell currents obtained from a rENaC expressing 3T3 cell dialyzed with a pipette solution containing 2 mM AMP. Currents were elicited by 800-ms voltage ramp between −144 and −4 mV from a holding potential of −44 mV every 30 s. *B*, time course of changes in amiloride-sensitive current amplitude at −104 mV from cells dialyzed with a pipette solution containing 2 mM AMP. *C*, effects of dialysis of the cells with a pipette solution containing ADP, AMP, GTP, and UTP at 2 mM each. The bath solution was a lithium glutamate-rich solution. For comparison, the amiloride-sensitive current values 5 min after whole-cell dialysis were normalized to those measured at 0 min at −104 mV. Initial amiloride-sensitive current at −104 mV was −1.50 ± 0.24 nA (n = 16), −1.54 ± 0.24 nA (n = 13), −2.05 ± 0.19 nA (n = 14), −2.05 ± 0.30 nA (n = 14), −1.56 ± 0.22 nA (n = 19), or −1.91 ± 0.25 nA (n = 14) when the cells were dialyzed with a solution containing no nucleotides (−), 2 mM ATP, 2 mM ADP, 2 mM AMP, 2 mM GTP, or 2 mM UTP, respectively. Shown are mean ± S.E.

TABLE I
Summary of single channel conductance obtained in outside-out patch experiments, where the patch pipette was filled with test solutions described

Test solutions	Single channel conductance
No nucleotide	8.2 ± 0.3 pS (n = 12)
ATP (10 mM)	7.9 ± 0.5 pS (n = 8)
ATP (10 mM) + 10 mM EDTA	8.3 ± 0.6 pS (n = 7)
ADP (2 mM)	7.8 ± 0.3 pS (n = 6)
ATPγS (2 mM)	7.6 ± 0.3 pS (n = 3)
AMP-PNP (2 mM)	7.9 ± 0.4 pS (n = 5)
UTP (2 mM)	9.2 ± 0.1 pS (n = 3)
GTP (2 mM)	8.9 ± 0.2 pS (n = 4)

cell currents several minutes after whole-cell dialysis, thus we likely missed the relatively fast run down in MDCK cells. As shown in Fig. 9*A*, when the cells were dialyzed with a cesium glutamate pipette solution containing no ATP, amiloride-sensitive current ran down. The normalized amiloride-sensitive current amplitude within 5 min after whole-cell dialysis was decreased to 54.0 ± 10.2% (n = 11) of the initial amiloride-sensitive current level (Fig. 9*C*). The run down of the current was inhibited by dialysis of the cells with a pipette solution containing 2 mM ATP (92.5 ± 7.4% (n = 10)) or 2 mM AMP-PNP (99.5 ± 13.8% (n = 9) (Fig. 9*B*), but not 2 mM ADP (55.4 ± 6.5% (n = 11)) or 2 mM AMP (53.3 ± 10.1 (n = 8)) (Fig. 9*C*). These results suggest that the ATP regulation of rENaC is not confined to NIH-3T3 cells expressing ENaC but is also observed in epithelial cells and thus may represent a more generalized phenomenon of ENaC regulation in mammalian cells.

Binding of ATP to αrENaC—The above results collectively suggest that ATP may bind rENaC, possibly directly. Because αrENaC, but not β- or γrENaC, possess two putative nucleotide-binding (NB) sites (G*X*G*X*G and G*X*G*XX*G at the N and C termini, respectively), we tested if ATP can bind αrENaC. We thus incubated lysate of MDCK cells stably expressing αrENaC, either alone or together with βγ-rENaC, with immobilized (agarose-conjugated) ATP or AMP (used as a control). As shown in Fig. 10, the ATP-agarose beads, but not the AMP-agarose beads, were able to precipitate αrENaC from MDCK cell lysate. Similar results were obtained with several types of beads conjugated to ATP or AMP via different linkages and spacer lengths (C-8 attachment, 9 atom spacer; N-6 attachment, 11 atom spacer; ribose attachment, 11 atom spacers) (Fig. 10 and data not shown). Our preliminary data also indicate that binding of αrENaC to ATP-agarose can be competed off with soluble ATP (not shown). Thus, these results demonstrate binding of ATP, but not AMP, to αrENaC.

To test whether the putative NB motifs in αrENaC are indeed the binding sites for ATP, we generated stable MDCK cell lines expressing αrENaC mutated for both NB sites (Fig. 11*A*). As can be seen in Fig. 11*B*, mutating both NB motifs led to severe inhibition of ATP binding to αrENaC, implicating these motifs as major binding sites for ATP. Residual binding is still observed, however, in these mutants, suggesting that another minor binding site(s), not yet identified, may be involved

as well. We have also generated MDCK cell lines expressing individual NB motifs mutant (*i.e.* mutated NB motif in either the N or C terminus of αrENaC). Each of these revealed only partial inhibition of ATP binding (~40–60%), suggesting that both motifs are able to bind ATP under our experimental conditions (data not shown).

DISCUSSION

By using patch clamp techniques, we have shown here that rENaC heterologously expressed in both NIH-3T3 fibroblasts and MDCK epithelial cells is regulated by cytosolic ATP. This regulation is likely mediated by non-hydrolyzable nucleotide binding to rENaC itself (most likely) or to an accessory protein, rather than by a hydrolytic mechanism. To our knowledge, this is the first demonstration of ATP binding to rENaC and of cytosolic ATP-mediated regulation of rENaC expressed in mammalian cells.

In the present whole-cell patch clamp studies, we provide several lines of evidence that the sustained activity of rENaC expressed in 3T3 cells is dependent upon cytosolic ATP. (i) Whole-cell dialysis with an ATP-free pipette solution caused a marked run down of the whole-cell currents attributable to rENaC activity (Fig. 3). (ii) The run down was prevented when the pipette solution contained 2 mM ATP (Fig. 3). (iii) ATP prevented the run down in a dose-dependent manner (Fig. 4). Furthermore, because other nucleotides including ADP, AMP, GTP, or UTP at 2 mM were relatively ineffective (Fig. 6), the sustained activity of the rENaC in 3T3 cells seems to be regulated by ATP itself rather than by other nucleotides. Moreover, a similar run down of the amiloride-sensitive whole-cell currents was observed in MDCK cells expressing rENaC, and this run down was also inhibited by ATP, but not by ADP or AMP (Fig. 9), arguing against the possibility that ATP regulation of rENaC in 3T3 cells is a peculiar phenomenon specific to 3T3 cells.

Under the present experimental conditions, the whole-cell current attributable to rENaC activity ran down and reached a steady-state level within 4–5 min after onset of whole-cell dialysis. The time course of the run down should depend upon the rate of diffusional equilibrium of ATP in 3T3 cells, because the time course of dialysis between the patch pipette and the cell interior is a function of cell volume and geometry, access resistance between the pipette and the cell, and the molecular weight of the molecules tested (36). Furthermore, in the whole-cell experiments, the local concentration of ATP in the proximity to rENaC (or its putative regulatory protein) may not be exactly the same as in the pipette due to diffusion limitations and endogenous ATP production and consumption. Therefore, the present study does not allow us to determine the precise K_d value of ATP for rENaC activity. Nevertheless, the data are consistent with the idea that relatively high ATP concentrations, in the millimolar range, are required to maintain maximal activity of rENaC. This idea is also supported by the present outside-out patch experiments, demonstrating that cytosolic ATP at millimolar concentrations could prevent the run down of rENaC activity.

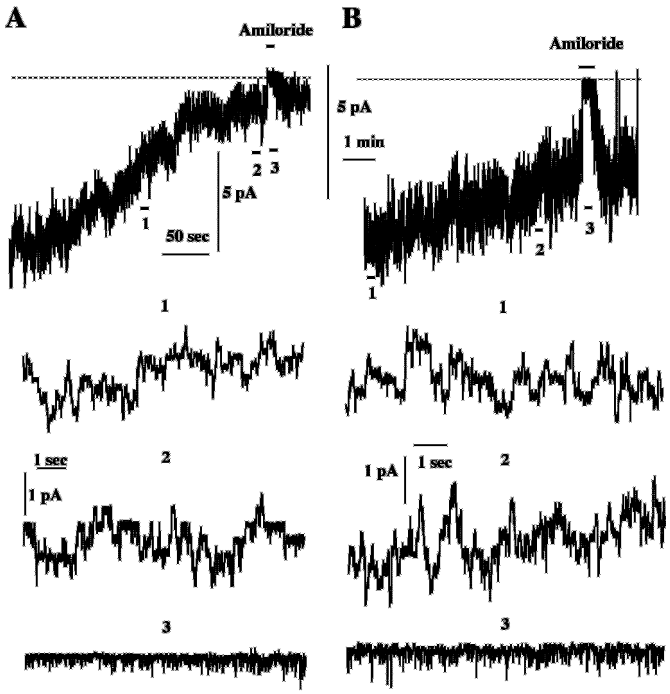

FIG. 7. **Stability of rENaC activity in excised outside-out patches with pipette solution without or with ATP.** No ATP (*A*) or 2 mM ATP (*B*) was included in the pipette solution, and the bath solution contained a lithium glutamate-rich solution. As soon as whole-cell configuration was established, the membrane was excised to make outside-out patches. Channel activity was continuously recorded at −24 mV for more than 5 min. Application of amiloride (10 μM, *thick bar*) to the bath solution abolished channel activity. The *top trace* shows the time course of the amiloride effect. Three parts of the trace (*1–3*) are extended to display the details of the channel activity. Holding potential was −24 mV.

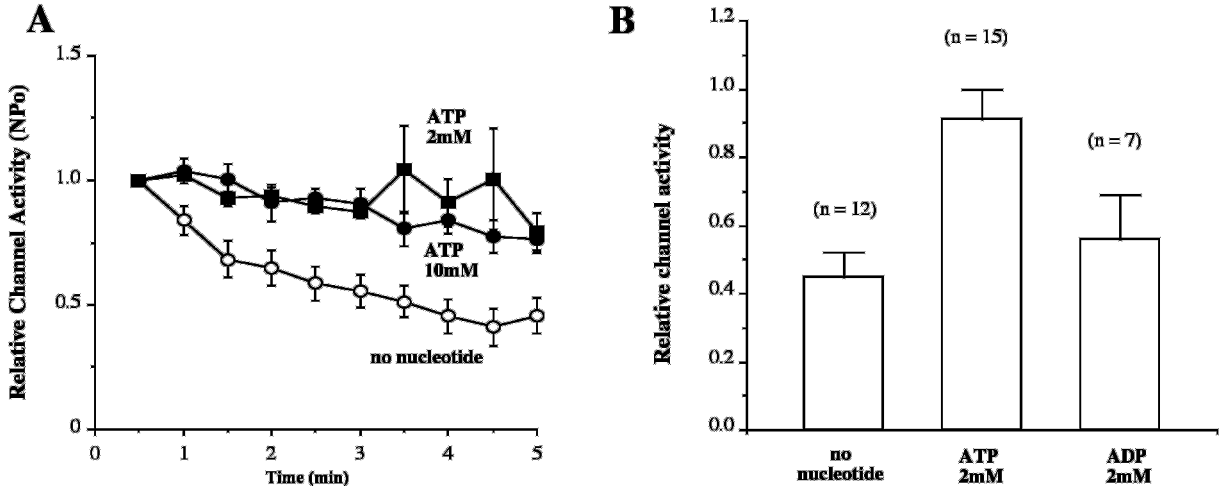

FIG. 8. *A*, time course of the changes in the relative channel activity (NP_o). NP_o value was estimated every 30 s and normalized to 1 with the initial 30 s. Data were obtained from 12, 15, or 10 experiments. *B*, summary of the effects of cytosolic ATP and ADP (2 mM) on the stability of channel activity. Data were obtained from 12, 14, or 7 experiments, respectively.

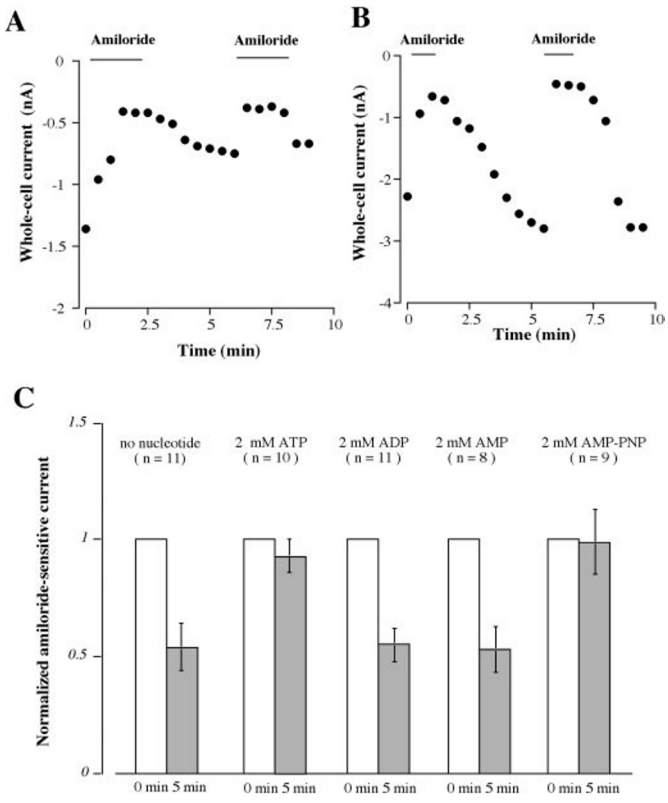

FIG. 9. Representative experiments showing the effect of dialysis of rENaC-expressing MDCK cells with a pipette solution containing either (*A*) no nucleotide or (*B*) 2 mM AMP-PNP on the amiloride-sensitive currents. The whole-cell current at −104 mV was measured every 0.5 min. Currents were elicited by 400-ms voltage ramp between −104 and +16 mV from a holding potential of −44 mV. *C,* summary of the effects of dialysis of rENaC-expressing MDCK cells with a pipette solution containing either no nucleotide or 2 mM ATP, ADP, AMP, and AMP-PNP on the amiloride-sensitive currents. Currents were elicited by 400-ms voltage ramp between −104 and +16 mV from a holding potential of −44 mV. For comparison, the amiloride-sensitive current values 5 min after whole-cell dialysis were normalized to those measured at 0 min at −104 mV. Initial amiloride-sensitive current at −104 mV was −3.07 ± 1.03 nA (n = 11), −2.75 ± 0.56 nA (n = 10), −4.60 ± 0.44 nA (n = 11), −3.32 ± 0.95 nA (n = 8), and −3.32 ± 0.84 nA (n = 9) when the cells were dialyzed with a solution containing no nucleotides, 2 mM ATP, 2 mM ADP, 2 mM AMP, and 2 mM AMP-PNP, respectively. Shown are mean ± S.E.

The run down of ENaC activity in the conventional whole-cell experiments has been also reported in cortical collecting tubule cells freshly isolated from rats maintained on a low sodium diet (33). These investigators observed that whole-cell dialysis of the cells caused a rapid fall in whole-cell currents mediated by ENaC within the first 5 min of their whole-cell recording. Although the kinetics of the run down seen in these cells was similar to that in the present study, the underlying mechanism appears to be different, because it was prevented by 0.3 mM GDPβS but not by ATP (3 mM), ADP (3 mM), GTP (0.3 mM), GDP (0.3 mM), or GTPγS (0.3 mM) (34). Currently, we do not have an explanation for the differences between these results and ours.

As the macroscopic whole-cell conductance mediated by ENaC is defined as a product of single channel conductance (g), the number of active channels (N), and open probability (P_o), the run down of the macroscopic conductance should be attributable to the decrease in these parameters. In excised outside-out patch experiments, we showed that single channel conductance was not changed in experiments where the cytosolic surface of the membrane was exposed to various experimental solution used in the whole-cell experiments (Table I). These results suggest that alternation of single channel conductance

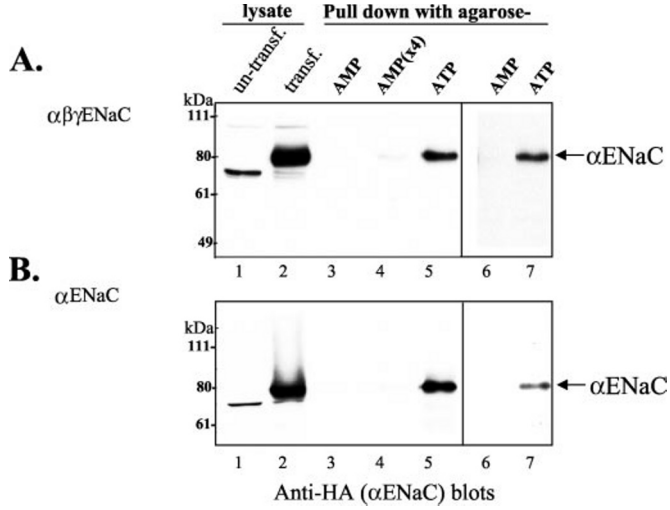

FIG. 10. **Binding of ATP to αrENaC.** ATP- or AMP-agarose beads were incubated with diluted lysate from MDCK cells stably expressing rat all-tagged ENaC ($\alpha_{HA}\beta_{myc.T}\gamma_{Flag}$-ENaC) (*A*) or rat HA-αrENaC alone (*B*). Beads were then extensively washed, and bound protein was separated on a 7% SDS-PAGE and immunoblotted with anti-HA antibodies to detect αrENaC. *Lanes 1* and *2* depict untransfected (*un-transf*) and ENaC-expressing MDCK cells, respectively. *Lanes 3–5* represent pull down experiments with C-8 attached (9 atom spacer) AMP- or ATP-agarose beads, where AMP and ATP concentrations are equal (90 nmol in 1.5 ml diluted lysate) in *lanes 3* and *5*, and 4 times AMP (360 nmol) used in *lane 4* (to equate the volume of agarose beads to that of the agarose-ATP in *lane 5*). *Lanes 6* and *7* represent pull down experiments with equal concentrations of ribose-attached (11 atom spacer) AMP- or ATP-agarose beads (90 nmol in 1.5 ml., and where beads volume of the AMP beads was 2.5 times that of the ATP beads). Exposure time of the film in *lanes 6* and *7* (in *A* and *B*) was longer than in *lanes 3–5.* The ~70-kDa band seen in *lane 1* (untransfected MDCK cell lysate) is a nonspecific band cross-reacting with the anti-HA antibodies.

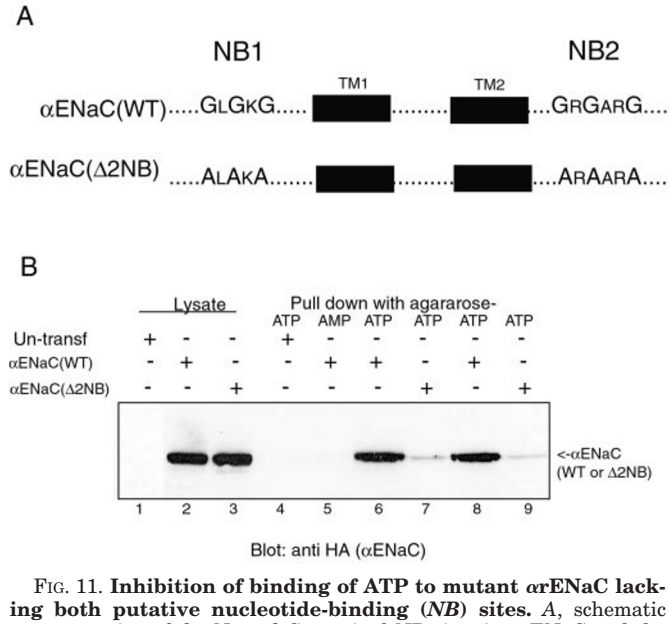

FIG. 11. **Inhibition of binding of ATP to mutant αrENaC lacking both putative nucleotide-binding (*NB*) sites.** *A*, schematic representation of the N- and C-terminal NB sites in αrENaC and the mutant bearing Gly → Ala mutations in all glycines of the NB sites (HA-αrENaC(Δ2NB)). *B*, ATP-agarose beads were incubated with diluted lysate from MDCK cells either untransfected (*un-transf*, *lane 4*) or stably expressing wild type HA-αrENaC (*WT*) (*lanes 6* and *8*) or HA-αrENaC(Δ2NB) (*lanes 7* and *9*). Beads were then extensively washed, and bound protein was separated on a 10% SDS-PAGE and immunoblotted with anti-HA antibodies to detect αrENaC. AMP-agarose beads were also used as controls (*lane 5*). *Lanes 1–3* depict lysates from untransfected (*un-transf*), WT, and Δ2NB mutants cells used for the experiment. *Lanes 6–9* represent duplicate treatments.

is not involved in the run down of the macroscopic ENaC currents. Furthermore, in excised outside-out patch experiments, we also found that cytosolic ATP, but not ADP (each at 2 mM), was effective in preventing the run down of channel activity (Fig. 8). Assuming a fixed number of channels in excised outside-out patches (as insertion or degradation of ENaC is unlikely to take place in such excised membranes), these results suggest that a decrease in the overall open probability of ENaC present at the membrane may be responsible for the run down of the macroscopic currents. Therefore, we conclude that a decrease of the channel activity, defined as NP_o, is responsible for the run down of the macroscopic currents.

Our data are compatible with the hypothesis that the effect of ATP on ENaC is mediated through non-hydrolytic binding to ENaC, most likely by association with αENaC, rather than through ATP hydrolysis and phosphorylation. The hypothesis is strongly supported by the following observations. (i) ATP was effective in preventing the run down without Mg^{2+}, a cofactor required for ATP hydrolysis and phosphorylation (Fig. 5). (ii) The non-hydrolyzable ATP analogues AMP-PNP and ATP-γS, at 2 mM, were able to prevent the run down (Figs. 5 and 9). (iii) The approximate K_d value of the ATP effect was close to the mM range (Fig. 4). (iv) Binding experiments using agarose-conjugated ATP or AMP beads demonstrated association of αENaC with ATP but not AMP beads (Fig. 10). In this regard, it is noteworthy that there are two consensus nucleotide-binding motifs in αrENaC: an N-terminal Gly-*X*-Gly-*X*-Gly sequence found in αrENaC as also seen in the Cl^- channel Icln (37), and a C-terminal Gly-*X*-Gly-*X*-*X*-Gly motif that is conserved in αENaC of several species as well as in most protein kinases (38). Indeed, mutating those motifs in αENaC inhibits ATP binding (Fig. 11), lending further support to the notion that ATP directly binds αENaC. At present, however, we do not know how binding of ATP to ENaC may regulate channel activity, although we can speculate it may alter channel conformation, in some way affecting its activity.

Our data may give an explanation for a previous observation that when co-expressed with the β- and γENaC subunits in *Xenopus* oocytes, a splice variant of αENaC lacking 49 amino acids in the N-terminal region produced a considerably smaller amiloride-sensitive Na^+ current than wild type, a reduction of the currents being attributable to a decrease in the overall open probability of activity channels (25). The 49-amino acid deletion at the N terminus of αENaC removing the ATP-binding site may lead to reduced ENaC activity (*i.e.* decreased open probability), possibly by permanently locking the channel in a "run down" state, although we cannot exclude the possibility that other region(s) within these 49 amino acids is (are) also contributing to the effect. In fact, our experiments on a nucleotide-binding motif mutant in the N terminus of αENaC revealed a partial inhibition of ATP binding. Furthermore, the splice variant, which is shown to be expressed in various tissues expressing the normal ENaC (25), might play a role in diversity of the regulation of ENaC in native tissues.

Abriel and Horisberger (18) showed that perfusion of the cytoplasm with or without ATP had no effect on the activity of rENaC heterologously expressed in *Xenopus* oocytes using the "cut open oocyte" technique, leading them to suggest that direct interactions of ATP and the ENaC protein itself are unlikely. At this stage, we do not have a simple way to account for the differences between their results and ours. It may be that an unknown component(s), washed away by the rigorous intracellular perfusion in the cut open oocyte system, is needed for the ATP-ENaC association and the ensuing regulation of channel activity by ATP. Although our results strongly suggest a direct binding of ATP to ENaC, indirect binding cannot be precluded at present. In this regard, it is interesting to note a previous study demonstrating that glibenclamide, a known inhibitor of ATP-binding cassette proteins, such as CFTR or the sulfonylurea receptor, induced amiloride-sensitive currents in oocytes expressing human or *Xenopus* ENaC but not rENaC (39). These authors suggested the possibility of an existence of an ATP-binding cassette-type regulatory protein closely associated with ENaC in *Xenopus* oocytes

Although the present study was undertaken in heterologous expression systems (NIH-3T3 fibroblasts and MDCK epithelial cells), our data clearly suggest that the activity of ENaC can be under the control of cytosolic ATP in native cells. It has been shown in tight epithelia that the rate-limiting step for transepithelial Na^+ absorption is Na^+ entry through ENaC across the apical membrane, and that Na^+-K^+-ATPase adapts its activity to maintain a low intracellular Na^+ concentration (1). Taking into account the fact that the Michaelis-Menten constant of the Na^+-K^+-ATPase for ATP is very low (40), only a drastic depletion of ATP would be able to affect this pump. If regulation of ENaC by intracellular ATP levels was to take place in native epithelial cells, it would effectively prevent the overloading of Na^+ in these cells under certain metabolic stress conditions, in addition to the regulation provided by membrane potential and by cytosolic Na^+. Furthermore, assuming cytosolic ATP concentrations in the mM range, the ATP-mediated regulation of ENaC reported in the present study could be also important for the fine-tuning of ENaC activity.

REFERENCES

1. Garty, H., and Palmer, L. G. (1997) *Physiol. Rev.* **77,** 359–396
2. Canessa, C. M., Horisberger, J.-D., and Rossier, B. C. (1993) *Nature* **361,** 467–470
3. Canessa, C. M., Schild, L., Buell, G., Thorens, B., Gautschi, I., Horisberger, J.-D., and Rossier, B. C. (1994) *Nature* **367,** 463–467
4. Chang, S. S., Gruender, S., Hanukoglu, A., Roesler, A., Mathew, P. M., Hanukoglu, I., Schild, L., Lu, Y., Shimkets, R. A., Nelson-Williams, C., Rossier, B. C., and Lifton, R. P. (1996) *Nat. Genet.* **12,** 248–253
5. Strautnieks, S. S., Thompson, R. J., Gardiner, R. M., and Chung, E. (1996) *Nat. Genet.* **13,** 248–250
6. Grunder, S., Firsov, D., Chang, S. S., Jaeger, N. F., Gautschi, I., Schild, L., Lifton, R. P., and Rossier, B. C. (1997) *EMBO J.* **16,** 899–907
7. Shimkets, R. A., Warnock, D. G., Bositis, C. M., Nelson-Williams, C., Hansson, J. H., Schambelan, M., Gill, J. R., Ulick, S., Milora, R. V., Findling, J. W., Canessa, C. M., Rossier, B. C., and Lifton, R. P. (1994) *Cell* **79,** 407–414
8. Hansson, J. H., Schild, L., Lu, Y., Wilson, T. A., Gautschi, I., Shimkets, R., Nelson-Williams, C., Rossier, B. C., and Lifton, R. P. (1995) *Proc. Natl. Acad. Sci. U. S. A.* **92,** 11495–11499
9. Hansson, J. H., Nelson-Williams, C., Suzuki, H., Schild, L., Shimkets, R., Lu, Y., Canessa, C., Iwasaki, T., Rossier, B. C., and Lifton, R. P. (1995) *Nat. Genet.* **11,** 76–82
10. Stutts, M. J., Canessa, C. M., Olsen, J. C., Hamrick, M., Cohn, J. A., Rossier, B. C., and Boucher, R. C. (1995) *Science* **269,** 847–850
11. Stutts, M. J., Rossier, B. C., and Boucher, R. C. (1997) *J. Biol. Chem.* **272,** 14037–14040
12. Mall, M., Hipper, A., Greger, R., and Kunzelmann, K. (1996) *FEBS Lett.* **381,** 47–52
13. Mall, M., Bleich, R., Greger, R., Schreiber, R., and Kunzelmann, K. (1998) *J. Clin. Investig.* **102,** 15–21
14. Hummler, E., Barker, P., Gatzy, J., Beermann, F., Verdumo, C., Schmidt, A., Boucher, R. C., and Rossier, B. C. (1996) *Nat. Genet.* **12,** 325–328
15. Kellenberger, S., Gautschi, I., Rossier, B. C., and Schild, L. (1998) *J. Clin. Investig.* **101,** 2741–2750
16. Ishikawa, T., Marunaka, Y., and Rotin, D. (1998) *J. Gen. Physiol.* **111,** 825–846
17. Chalfant, M. L., Denton, J. S., Berdiev, B. K., Ismailov, I. I., Benos, D. J., and Stanton, B. A. (1999) *Am. J. Physiol.* **276,** C477–C486
18. Abriel, H., and Horisberger, J.-D. (1999) *J. Physiol. (Lond.)* **516,** 31–43
19. Chabot, H., Vives, M. F., Dagenais, A., Grygorczyk, C., Berthiaume, Y., and Grygorczyk, R. (1999) *J. Membr. Biol.* **163,** 175–188
20. Awayda, M. S. (1999) *Am. J. Physiol.* **277,** C216–C224
21. Palmer, L. G., Edelman, I. S., and Lindemann, B. (1980) *J. Membr. Biol.* **57,** 59–71
22. Garty, H., Edelman, I. S., and Lindemann, B. (1983) *J. Membr. Biol.* **74,** 15–24
23. Frindt, G., Silver, R. B., Windhager, E. E., and Palmer, L. G. (1995) *Am. J. Physiol.* **268,** F480–F489
24. Stutts, M. J., Gatzy, J. T., and Boucher, R. C. (1988) *J. Appl. Physiol.* **64,** 253–258
25. Chraïbi, A., Verdumo, C., Mérillat, A.-M., Rossier, B. C., Horisberger, J.-D., and Hummler, E. (2001) *Cell. Physiol. Biochem.* **11,** 115–122
26. Staub, O., Dho, S., Henry, P. C., Correa, J., Ishikawa, T., McGlade, J., and Rotin, D. (1996) *EMBO J.* **15,** 2371–2380
27. Hanwell, D., Ishikawa, T., Saleki, R., and Rotin, D. (2002) *J. Biol. Chem.* **277,**

9772–9779
28. Hamill, O. P., Marty, A., Neher, E., Sakmann, B., and Sigworth, F. S. (1981) *Pfluegers Arch.* **391,** 85–100
29. Barry, P. H., and Lynch, J. W. (1991) *J. Membr. Biol.* **121,** 101–117
30. Awayda, M. S., Ismailov, I. I., Berdiev, B. K., Fuller, C. M., and Benos, D. J. (1996) *J. Gen. Physiol.* **108,** 49–65
31. Hilgemann, D. W. (1997) *Annu. Rev. Physiol.* **59,** 193–220
32. Bond, T., Basavappa, S., Christensen, M., and Strange, K. (1999) *J. Gen. Physiol.* **113,** 441–456
33. Frindt, G., and Palmer, L. G. (1996) *Am. J. Physiol.* **271,** F1086–F1092
34. Palmer, L. G., Sackin, H., and Frindt, G. (1998) *J. Physiol. (Lond.)* **509,** 151–162
35. Mirshahi, M., Mirshahi, S., Golestaneh, N., Nicolas, C., Mishal, Z., Lounes, K. C., Hecquet, C., Dagonet, F., Pouliquen, Y., and Agarwal, M. K. (2001) *Ophthalmic Res.* **33,** 7–19
36. Pusch, M., and Neher, E. (1988) *Pfluegers Arch.* **411,** 204–211
37. Paulmichl, M., Li, Y., Wickman, K., Ackerman, M., Peralta, E., and Clapham, D. (1992) *Nature* **356,** 238–241
38. Hanks, S. K., Quinn, A. M., and Hunter, T. (1988) *Science* **241,** 42–52
39. Chraïbi, A., and Horisberger, J.-D. (1999) *J. Pharmacol. Exp. Ther.* **290,** 341–347
40. Jorgensen, P. L. (1980) *Physiol. Rev.* **60,** 864–917